Characterization of BphF, a Rieske-Type Ferredoxin with a Low Reduction Potential†

Manon M.-J. Couture,‡ Christopher L. Colbert,§ Elena Babini,‡,|| Federico I. Rosell,⊥ A. Grant Mauk,⊥ Jeffrey T. Bolin,§ and Lindsay D. Eltis*,‡,⊥,#

Department of Biochemistry, Université Laval, Québec, Canada, G1K 7P4, Department of Biological Sciences, Purdue University, West Lafayette, IN 47907-1392, Department of Biochemistry, University of British Columbia, Vancouver, British Columbia, Canada, V6T 1Z3, and Department of Microbiology and Immunology, University of British Columbia, Vancouver, British Columbia, Canada, V6T 1Z3

Received July 28, 2000; Revised Manuscript Received October 24, 2000

ABSTRACT: BphF is a small, soluble, Rieske-type ferredoxin involved in the microbial degradation of biphenyl. The rapid, anaerobic purification of a heterologously expressed, his-tagged BphF yielded 15 mg of highly homogeneous recombinant protein, rcBphF, per liter of cell culture. The reduction potential of rcBphF, determined using a highly oriented pyrolytic graphite (HOPG) electrode, was −157 ± 2 mV vs the standard hydrogen electrode (SHE) (20 mM MOPS, 80 mM KCl, and 1 mM dithiothreitol, pH 7.0, 22 °C). The electron paramagnetic resonance spectrum of the reduced rcBphF is typical of a Rieske cluster while the close similarity of the circular dichroic (CD) spectra of rcBphF and BedB, a homologous protein from the benzene dioxygenase system, indicates that the environment of the cluster is highly conserved in these two proteins. The reduction potential and CD spectra of rcBphF were relatively independent of pH between 5 and 10, indicating that the pK_as of the cluster's histidinyl ligands are not within this range. Gel filtration studies demonstrated that rcBphF readily oligomerizes in solution. Crystals of rcBphF were obtained using sodium formate or poly(ethylene glycol) (PEG) as the major precipitant. Analysis of the intermolecular contacts in the crystal revealed a head-to-tail interaction that occludes the cluster, but is very unlikely to be found in solution. Oligomerization of rcBphF in solution was reversed by the addition of dithiothreitol and is unrelated to the noncovalent crystallographic interactions. Moreover, the oligomerization state of rcBphF did not influence the latter's reduction potential. These results indicate that the 450 mV spread in reduction potential of Rieske clusters of dioxygenase-associated ferredoxins and mitochondrial bc_1 complexes is not due to significant differences in their solvent exposure.

Proteins containing iron−sulfur centers are widely distributed in nature, playing roles in many fundamental biological processes such as electron transfer, catalysis, and the regulation of both gene expression and protein function (*1*). Several different types of iron−sulfur proteins have been identified, the best studied being those that contain a single Fe atom ligated by four cysteinyl residues and those that contain [Fe_2S_2] or [Fe_4S_4] clusters. Spectroscopic, electrochemical, and structural studies of model compounds as well as wild-type and mutationally altered biological systems have contributed tremendously to our understanding of these proteins and their redox-active centers. Nevertheless, many factors governing the properties of iron−sulfur clusters have yet to be fully elucidated and research in this field remains very active, especially with respect to the influence of the protein structure on the redox properties of the clusters (*2*).

Among various iron−sulfur clusters involved in electron transfer is the "Rieske-type" [Fe_2S_2] cluster. First discovered in 1964 by Rieske and co-workers (*3*) in the bovine heart mitochondrial bc_1 complex, it has since been identified in bacterial bc_1 complexes (*4*, *5*), in various photosynthetic complexes (*6*) and in aromatic ring-dihydroxylating dioxygenases of bacteria (*7*). In the oxidized form, both Fe atoms in the Rieske cluster are in the ferric state. One Fe is readily reduced, with a reduction potential between +360 and −160 mV vs SHE.[1] The redox-active Fe is ligated to two histidinyl ligands whereas the other Fe is bound by two cysteinyl thiolates (*7*−*13*). In contrast, the [Fe_2S_2] clusters in "plant-type" ferredoxins are ligated by four cysteinyl residues and

† This work was supported in part by operating grant OGP0171359 from the NSERC of Canada (to L.D.E.), MRC of Canada Grant MT-7182 (to A.G.M.), and NIH Grant GM52381 (to J.T.B.). M.M.J.C. is the recipient of a studentship from the FCAR of Quebec, Canada. C.L.C. was supported in part by institutional training award GM-08296 from the NIH.

* To whom correspondence should be addressed. Phone: (604) 822-0042. Fax: (604) 822−6041. E-mail: leltis@interchange.ubc.ca.

‡ Université Laval.

§ Purdue University.

|| Present address: Institute of Agricultural Chemistry, University of Bologna, 40127 Bologna, Italy.

⊥ Department of Biochemistry, University of British Columbia.

Department of Microbiology and Immunology, University of British Columbia

[1] Abbreviations: CAPS, cyclohexylaminopropane sulfonic acid; CD, circular dichroism; CHES, cyclohexylamino-ethane sulfonic acid; CV, cyclic voltammetry; DTT, dithiothreitol; EPR, electron paramagnetic resonance; HEPPS, *N*-2-hydroxyethylpiperazine-*N*′3-propanesulfonic acid; HOPG, highly oriented pyrolytic graphite; MES, 2-(*N*-morpholino)ethanesulfonic acid; MOPS, 3-(*N*-morpholino)-propanesulfonic acid; PEG, poly(ethylene glycol); rcBphF, recombinant BphF; SHE, standard hydrogen electrode; TAPS, *N*-tris-(hydroxymethyl)methyl-3-aminopropanesulfonic acid.

10.1021/bi001780r CCC: $20.00
Published on Web 12/12/2000

possess reduction potentials between −250 and −450 mV vs SHE. The EPR spectra of the reduced Rieske cluster has a typical g_{av} of 1.91 (*3*, *14*) compared to 1.96 for the [Fe_2S_2] center of plant-type ferredoxins (*15*). While these spectroscopic characteristics appear to be conserved in all Rieske clusters studied to date, important biophysical differences are observed between the clusters of the membrane-associated respiratory and photosynthetic proteins on one hand and those of microbial ring-dihydroxylating dioxygenases on the other.

Aromatic ring-dihydroxylating dioxygenases catalyze the first step in the microbial degradation of a broad range of aromatic compounds, including naphthalene, biphenyl, and benzene (*7*). This function requires a multicomponent system consisting of a short electron transfer chain that provides electrons to a very large (and usually multimeric) terminal oxygenase, which oxidizes the substrate to the corresponding *cis*-dihydrodiol in an active site that contains a mononuclear (ferrous) Fe atom in a non-heme, non-sulfur environment. The first member of the electron-transfer chain is a flavoprotein, which accepts electrons from a nicotinamide cofactor and may also contain a plant-type [Fe_2S_2] cluster. The ultimate reductant of the Fe(II) active site is a Rieske-type cluster, which is bound by a distinct domain of the oxygenase and has a reduction potential of approximately −115 mV (*16*, *17*). In many but not all cases, the electron transfer chain also includes a small, independent ferredoxin that carries a second Rieske-type cluster possessing a reduction potential of approximately −150 mV (*7*, *18*).

In contrast, the reduction potentials of the Rieske clusters in soluble protein fragments from the mitochondrial bc_1 and the photosynthetic b_6f complexes are approximately +315 mV vs SHE at pH 7.0 (*21*, *22*). This considerable difference in reduction potentials has been attributed primarily to variations in the locations of the clusters relative to the protein−solvent boundary (*18*, *19*). Indeed, the structural similarity of the mitochondrial bc_1 and the photosynthetic b_6f cluster binding domains is striking, and in both cases, the cluster is located very near the protein surface with the histidine ligands exposed (*12*, *13*). Further similarities include extremely comparable hydrogen-bonding networks, a disulfide bridge that buttresses one side of the cluster, and a "Proloop" that covers the other side of the cluster binding fold. The sequences of dioxygenase-associated Rieske proteins/domains contain neither the cysteines necessary for a disulfide bond nor the GPAP conserved sequence of the Proloop. Moreover, in the recently determined crystal structure of the terminal oxygenase component from naphthalene dioxygenase, the hydrogen-bonding scheme differs from that observed in the vicinity of the bc_1 and b_6f clusters, and the cluster is buried at a subunit interface where its histidinyl ligands are involved in hydrogen bonds with carboxylates from the non-Rieske domain of a different subunit (*17*). Thus, in the case of the Rieske ferredoxins, it was also reasonable to expect that the cluster is buried within the monomer (*18*) or by formation of an oligomer (*19*).

The *bphF* gene of *Burkholderia* sp. strain LB400 encodes a soluble ferredoxin of 12.1 kDa that functions in the electron-transfer chain of the ring-hydroxylating dioxygenase involved in the microbial degradation of biphenyl (*23*). This protein contains an [Fe_2S_2] Rieske-type cluster typical of aromatic ring-dihydroxylating dioxygenases. BphF transfers electrons from a flavin-containing reductase to the oxygenase component of biphenyl dioxygenase, the first enzyme of the biphenyl degradation pathway. We report here the expression, purification, and crystallization of recombinant (rc) BphF. The electrochemical, spectroscopic, and oligomeric properties of the protein were investigated. This work also contributed to determination of the crystallographic structure of rcBphF (*20*). The results are discussed in light of this structure, as well as the structure and function of other Rieske cluster-containing proteins.

EXPERIMENTAL PROCEDURES

Bacterial Strains and Plasmids. Strains used for protein expression or DNA propagation included *Escherichia coli* TOPP strains 1 and 6 (Stratagene), BL21(DE3) (*24*), BL21-(DE3):pLysS (*24*), NovaBlue (Novagen), NovaBlue(DE3), (Novagen) and LE392 (*25*). Plasmids used in this work were pT7-7 (*26*), pET28a$^+$ (Novagen), pA1A5 (*27*), and pLEHP20 (*28*). In experiments designed to test the expression of recombinant ferredoxin, bacterial strains were grown on terrific broth (TB, Difco) media supplemented with Goodies (*29*, *30*), 15 μg/mL carbenicillin, 15 μg/mL tetracyclin, and/or 25 μg/mL chloramphenicol as required. Bacterial strains used for other purposes were grown on LB supplemented with the appropriate antibiotics.

DNA Manipulation and Amplification. DNA was manipulated using standard protocols (*31*). The *bphF* gene of strain LB400 was amplified by the polymerase chain reaction (PCR) using the following primers: BPHF-For, 5′-GGGCAT-ATGAAATTTACCAGA-3′ and BPHF-Rev 5′-CGCCTG-CAGATGGTGTCGATCAT-3′. These primers were based on the published sequence of *bphF* (*23*) and introduce *Nde*I and *Pst*I restriction sites at the 5′ and 3′ ends, respectively, of the amplified product, thus facilitating subsequent cloning of the gene. The PCR contained 3.6 ng/μL of the template DNA, 5 units of TAQ DNA polymerase (Perkin-Elmer Cetus, Norwalk, CT), 0.2 nM of each dNTP, and 0.1 pmol/μL of each primer. Twenty-four temperature cycles were performed as follows: 96 °C for 15 s, 42 °C for 30 s, and 72 °C for 45 s. The PCR product was purified using a Magic PCR Prep kit (Promega).

Protein Purification. All buffers were made with water purified to a resistivity of greater than 17 MΩ cm on a NANOpure UV water purifier (Barnstead, Dubuque, Iowa). The pH was determined using a model PHM93 Reference pH Meter (Radiometer, Copenhagen). The protein purification and handling were performed under anaerobic conditions. All buffers were deoxygenated prior to use by bubbling them for 20 min with argon and equilibrating them for 24 h in an anaerobic environment (less than 1 ppm O_2). Protein concentration and buffer exchange were accomplished using Amicon stirred cell concentrators. Chromatographic procedures were performed with an ÄKTA Explorer purification system (Amersham Pharmacia Biotech, Baie d'Urfé, P. Q., Canada).

E. coli LE392 cells containing the plasmid pEBRE12 were grown at 37 °C for 24 h, harvested by centrifugation and stored at −80 °C until further use. Cells were resuspended in the lysis buffer (20 mM MOPS, 300 mM sodium chloride, 5 mM imidazole, 1 mM magnesium chloride, 1 mM calcium chloride, 200 units/mL DNase, and 1 unit/mL RNase, pH

8.0) and rapidly disrupted by two successive passages through a French Press cell precooled to 4 °C and operated at 20 000 psi. The cellular extract was then flushed with argon for 20 min and the cellular debris was removed by ultracentrifugation at 25 000 g for 1 h using sealed ultracentrifuge tubes. The supernatant was loaded onto a Ni^{2+}-chelating column, washed with 20 mM MOPS, 300 mM NaCl, 20 mM imidazole, pH 8.0, to remove nonspecifically bound contaminants, and eluted with 20 mM MOPS, 300 mM sodium chloride, 150 mM imidazole, pH 8.0.

The rcBphF was exchanged into a thrombin cleavage buffer (50 mM Tris-HCl, 150 mM sodium chloride, and 2.5 mM calcium chloride, pH 7.5) and incubated for 16 h at 20 °C with a 1:1000 ratio (w/w) of thrombin to remove the His-tag. The protein was then loaded onto a MonoQ anion-exchange HR 10/10 column (Amersham Pharmacia Biotech) equilibrated in 20 mM MOPS, pH 7.0, 1 mM dithiothreitol (DTT). The recombinant ferredoxin was eluted at a flow rate of 4 mL/min with a linear gradient of 120 to 300 mM sodium chloride in 125 mL. Fractions containing rcBphF were pooled, concentrated to less than 2 mL and loaded onto a Superdex 200 HL 26/60 gel filtration column (Amersham Pharmacia Biotech). The protein was eluted at a flow rate of 3 mL/min with 20 mM MOPS, 150 mM sodium chloride, pH 7.0, and 1 mM DTT. Fractions containing rcBphF were pooled, concentrated to approximately 30 mg/mL and frozen as pellets in liquid nitrogen.

Determination of Protein Purity and Concentration. SDS−PAGE in Tris/Tricine (*32*) was performed on a Bio-Rad MiniProtean II apparatus and stained with Coomassie Blue according to established procedures (*31*). Protein concentrations were determined by the Bradford assay using bovine serum albumin as a standard (*33*).

Determination of Molecular Weight. The relative molecular weight of the rcBphF subunit was estimated by SDS−PAGE using a calibration curve of the following molecular weight markers (Bio-Rad): myosin (M_r = 200 000), β-galactosidase (M_r = 116 250), phosphorylase b (M_r = 97 400), serum albumin (M_r = 66 200), ovalbumin (M_r = 45 000), carbonic anhydrase (M_r = 31 000), and trypsin inhibitor (M_r = 21 500). The relative molecular weight of the native protein was determined using a HiLoad 16/60 Superdex 75 gel filtration column (Amersham Pharmacia Biotech) operated at a flow rate of 1 mL/min. The elution buffer contained 20 mM MOPS, pH 7.0, and 0.15 M NaCl. A calibration curve was obtained using the following molecular weight markers (Bio-Rad): thyroglobin (M_r = 670 000), gamma globulin (M_r = 158 000), ovalbumin (M_r = 44 000), myoglobin (M_r = 17 000), and vitamin B-12 (M_r = 1350). Partition coefficients were calculated the using the equation

$$K_{av} = (V_e - V_o)/(V_t - V_o)$$

Determination of Iron and Sulfur. The iron content of purified rcBphF was determined using Ferene-S (Sigma) following the procedure of Haigler and Gibson (*34*). The acid-labile sulfur content of rcBphF was determined using *N*,*N*′-dimethyl-*p*-phenylenediamine (Sigma) (*35*). In the iron and sulfur assays, *Chromatium vinosum* HiPIP was used as a control.

UV−Vis Absorption and Circular Dichroism Spectra. The rcBphF protein was reduced or oxidized by adding a small excess of sodium dithionite or potassium ferricyanide, respectively. Excess oxidizing or reducing agent was removed by passing the protein over a short desalting column (P6-DG, Bio-Rad). UV−vis spectra were recorded using a Varian Cary 3 spectrophotometer equipped with a thermostated cuvette holder and a circulating, thermostated water bath. Spectra were recorded between 200 and 800 nm at 20 °C. CD spectroscopy was performed with a UV−vis Jasco model J-720 spectropolarimeter. Protein solutions were placed in a jacketed, cylindrical quartz cell (1 mm path), and temperature was regulated with a Neslab RTE111 water bath operated under computer control. Thermal stability was measured as described previously (*36*). Spectra were recorded between 180 and 800 nm with a 1 nm band width and a sensitivity of 20 mdeg.

Electron Paramagnetic Resonance Spectroscopy. EPR spectra of reduced rcBphF were recorded at 4 K using a Bruker model ESP300E spectrometer equipped with an HP5352B microwave frequency counter, an Oxford Instrument ESR900 continuous flow cryostat, and an Oxford Instrument model ITC-4 temperature controller.

Cyclic Voltammetry. Cyclic voltammetry of rcBphF was performed using a micro-cell based on the design described by Hagen (*37*). Cyclic voltammograms were recorded with a Princeton Applied Research model 263a potentiostat using a highly oriented parallel graphite (HOPG) working electrode (Atom Graph, NY) and a Ag/AgCl reference electrode (Bioanalytical Systems, West Lafayette, IN). The HOPG working electrode was cleaned immediately prior to each electrochemical experiment by being polished successively with three deagglomerated alpha alumina (1, 0.3, and 0.05 μm)/water slurries on a Mastertex polishing cloth (Buehler, Lake Bluff, IL), thoroughly rinsed with water, and sonicated for 30 s to remove excess alumina. The protein was diluted approximately 50-fold to a concentration of 100 μM in the specified buffer or in a Good's buffer solution containing 10 mM each of MES [2-(*N*-morpholino)ethanesulfonic acid], MOPS [3-(*N*-morpholino)propanesulfonic acid], HEPPS (*N*-2-hydroxyethylpiperazine-*N*′3-propanesulfonic acid), TAPS [*N*-tris-(hydroxymethyl)methyl-3-aminopropanesulfonic acid], CHES (cyclohexylamino-ethane sulfonic acid), and CAPS (cyclohexylaminopropane sulfonic acid). The pH was adjusted with NaOH. The latter solution provides buffering capacity over a wide range of pH. Several compounds were tested for their ability to promote electron transfer between rcBphF and the electrode, including polymixin, poly-L-lysine, and the aminoglycosides neomycin, streptomycin, and kanamycin. In some cases, morpholin and 4,4-bipyridyl disulfide were used as stabilizers. The reduction potentials reported herein were converted to the standard hydrogen electrode (SHE).

The reduction potential was determined as a function of temperature using a nonisothermal configuration. The temperature of the sample was regulated by thermojacketting the microcell and connecting it to a Lauda circulating water bath. The temperature of the protein solution was monitored with a type T thermocouple connected to a model AN2402 Monitor/Controller (BJ Wolfe Enterprises, Agoura Hills, CA). CV measurements were performed when the sample temperature was within 0.2 °C of the target temperature. At each temperature, a new droplet of solution and a freshly prepared working electrode were used.

Crystallization of rcBphF. All crystallization procedures were performed anaerobically within a nitrogen atmosphere glovebox (Innovative Technology) maintained at ≤2 ppm O_2. An initial search for possible crystallization conditions was performed at 10 and 25 °C using the vapor diffusion method and Crystal Screen kits I and II from Hampton Research. Several potentially productive conditions were identified, but subsequent experiments established that the most reproducible crystal growth occurred with 4.0 M sodium formate or with 25−35% (w/v) poly(ethylene glycol) augmented with ammonium sulfate as the crystallizing agent. The diffraction data reported below are from a crystal grown by sitting drop vapor diffusion at 10 °C using a reservoir solution that contained 35% poly(ethylene glycol) monomethyl ether 5000, 0.2 M ammonium sulfate, and 0.1 M MES buffer, pH 6.0. To initiate the experiment, 3 μL of the reservoir solution was added to 3 μL of a solution that contained 31 mg/mL rcBphF, 0.150 M sodium chloride, 1 mM DTT, and 20 mM MOPS buffer, pH 7.0. Prior to diffraction experiments the crystal was serially transferred into anaerobic solutions containing the initial reservoir solution supplemented with 5, 10, 15, and 20% glycerol (ca. 2 min incubation per step). The crystal was extracted from the final solution in a loop mount and frozen by immediate immersion in liquid N_2.

X-ray Data Collection and Analysis. X-ray diffraction patterns were obtained by the use of CuKα radiation from a Rigaku rotating anode X-ray generator operated at ca. 50 kV and 100 mA and equipped with focusing mirror optics (Molecular Structures Corp.). Diffraction patterns from frozen crystals were recorded by the oscillation method and the use of an R-axis IV imaging plate detector system (Molecular Structures Corp.) equipped with a Cryostream crystal cooling device (Oxford Cryosystems, U.K.). The oscillation range and exposure time per frame were 1° and 10 min, respectively, the typical crystal to detector distance was 19.5 cm, and the temperature of the N_2 gas stream surrounding the crystal was maintained at a nominal value of 100 K. The patterns were analyzed, and the intensity measurements were scaled, postrefined, and merged by the use of the HKL software package (*38*). The CCP4 package (*39*) was used for additional crystallographic calculations.

RESULTS

Construction of the Expression Vector. Amplification of the *bphF* gene from pAIA5 yielded a DNA fragment of 355 bp. This fragment was digested with *Pst*I and *Nde*I, extracted from agarose gel after electrophoresis, repurified using the QiaEX kit (Qiagen, Mississauga, Ont.) and then ligated into appropriately digested pT7-7 plasmid, producing the plasmid pEBRE10. The *bphF* gene was isolated from this vector on an *Nde*I/*Hin*dIII fragment and inserted into pET28a$^+$ plasmid (Novagen). This construction, named pEBRE11, placed the *bphF* gene immediately downstream of a sequence encoding a poly-histidine tag and a thrombin recognition site. To place the *bphF* gene under the control of a P_{lac} promoter, the *Nco*I/*Hin*dIII fragment of pEBRE11 encoding the His-tagged BphF was inserted into pLEHP20 (*28*), yielding pEBRE12.

Expression and Purification. Among the systems tested for the expression of rcBphF, the highest level of recombinant ferredoxin was obtained from *E. coli* LE392 containing the plasmid pEBRE12. rcBphF was purified to apparent homogeneity (Figure 1) using immobilized metal affinity, anion-exchange and gel filtration chromatographies. Proteolytic removal of the His-tag by thrombin produced a recombinant (rc) BphF that is extended by three residues (Gly-3, Ser-2, and His-1) at its N-terminal relative to the wild-type protein. The rcBphF thus possesses 112 amino acids and a relative molecular mass of 12.4 kDa, which corresponds to the apparent molecular mass of the band resolved by Tris/Tricine SDS−PAGE (Figure 1). A yield of 15 mg of pure protein/L of TB media was obtained. The ratios of polypeptide to iron and sulfur were 1:1.84 and 1:1.76, respectively. RcBphF was soluble at concentrations up to 4 mM and was stable at room temperature when handled anaerobically.

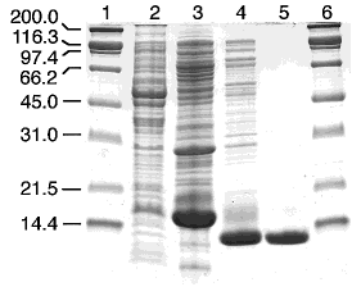

FIGURE 1: Coomassie-Blue stained SDS−polyacrylamide gel of rcBphF. The gel was loaded with protein standards (1 μg each, lanes 1 and 6) and the following preparations of rcBphF: crude extract (lane 2); the eluate from the Ni^{2+}-chelating column (lane 3); the eluate from the anion exchange column (lane 4); 10 μg of the eluate from the gel filtration column (lane 5). The separating gel contained 16.5% acrylamide.

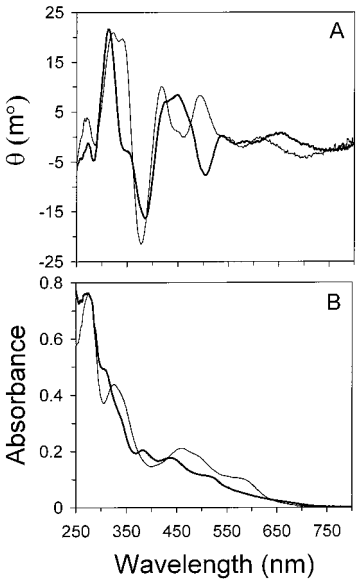

FIGURE 2: CD (A) and UV−vis absorption (B) spectra of oxidized (thin trace) and reduced (thick trace) rcBphF. The samples contained 50 μM rcBphF in 20 mM MOPS, 80 mM NaCl, pH 7.0 (25 °C).

UV−Vis Absorption and CD Spectroscopy. The electronic absorption spectra of reduced and oxidized rcBphF show broad, poorly resolved peaks in the UV−vis region that are typical of S → Fe(III) charge-transfer bands of iron sulfur proteins (Figure 2). The *R*-factor (A_{280}/A_{326}) of the purified oxidized protein was 1.65. The CD spectra of reduced and oxidized rcBphF exhibited bands that are similar in position

Table 1: Extinction Coefficients and Molar CD Absorptivities of rcBphF

absorption		CD	
λ (nm)	ϵ (mM^{-1} cm^{-1})	λ (nm)	$\Delta\epsilon$ (mdeg cm^2 M^{-1})
		oxidized	
326	9.0	323	+14.10
458	4.4	340	+13.29
492	3.8	377	−14.50
575	2.2	418	+6.80
		493	+5.54
		579	−1.51
		699	−2.87
		reduced	
308	9.3	312	+14.58
384	3.9	383	−10.84
436	3.4	422	+4.54
512	2.1	448	+5.62
		504	−5.16

[a] Values were determined in 20 mM MOPS and 80 mM NaCl, pH 7.0, 25 °C, and were calculated according to the iron content of the sample, as described in the text.

Table 2: Thermodynamic Parameters of the Reduction of rcBphF

$E°$ (mV)	−154.5
$\Delta S°$ (J mol^{-1} K^{-1})	−86.2
$\Delta G°$ (kJ mol^{-1})	14.9
$\Delta H°$ (kJ mol^{-1})	−10.8
$dE°/d\sqrt{I}$ (mV $M^{-1/2}$)	−52.9

[a] Values were determined as described in Experimental Procedures and are reported vs SHE. The temperature dependence was determined using a buffer that contained no DTT.

and intensity to those reported for the benzene dioxygenase ferredoxin component, BedB (*18*). Extinction coefficients and molar CD absorptivities based on the metal content of the protein are listed in Table 1.

The melting temperatures of the reduced (λ = 385 nm) and oxidized (λ = 378 nm) rcBphF were determined by CD spectroscopy to be 63.1 and 57.3 °C, respectively. Thermal denaturation of rcBphF was irreversible for both oxidation states.

Cyclic Voltammetry. Cyclic voltammetry was performed on rcBphF using an HOPG electrode. Of the compounds tested for their ability to promote electron transfer between rcBphF and the electrode, only neomycin promoted stable, quasi-reversible electron transfer as judged from the shape of the cyclic voltammograms and the separation between the anodic and cathodic peak currents (Figure 3).

With neomycin and potential sweep rates less than 50 mV/s, the intensities of the anodic and cathodic peak currents were directly proportional to the square root of the scan rate (results not shown). This linear relationship indicates that the electron transfer was quasi-reversible and diffusion-controlled under these conditions. At scan rates greater than 50 mV/s, the relationship deviated from linearity, indicative of a kinetic barrier for the electron-transfer process between rcBphF and the HOPG electrode. A scan rate of 10 mV/s was chosen for most subsequent electrochemical experiments. At this rate, the signal was stable for at least 30 scans. In investigating the pH dependence of the reduction potential, a scan rate of 5 mV/s was used as this gave a better signal over a broader pH range.

The midpoint reduction potential of rcBphF was −157 ± 2 mV vs SHE (20 mM MOPS, 80 mM KCl, and 1 mM DTT, pH 7.0, 22 °C), based on repetitive measurements performed over several weeks. At a scan rate of 10 mV/s, the separation between the anodic and cathodic peak currents was 65 mV (Figure 3). From these values, a heterogeneous rate constant $k° = 5.5 \times 10^3$ cm/s was calculated (*40*) by assuming that rcBphF has the same diffusion coefficient as those of BedB ferredoxin and the water-soluble fragment of the Rieske protein from the bc_1 complex (*18*). The reduction potential was also determined by spectrophotometrically monitored redox titration using an optically transparent thin layer electrode cell (*41*). A value of −152.4 mV vs SHE (20 mM MOPS and 80 mM NaCl, pH 7.0, 25 °C; results not shown) was obtained, which compares favorably to the value of −154.5 mV determined by CV under similar conditions (i.e., in a buffer that contained no DTT as described below).

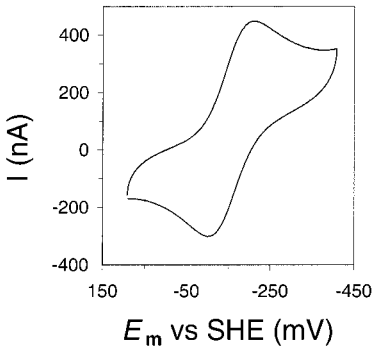

FIGURE 3: Cyclic voltammogram of rcBphF. The sample contained 100 μM rcBphF in 20 mM MOPS, 80 mM KCl, pH 7.0, 1 mM DTT, 2 mM neomycin at 22 °C. The cyclic voltammogram was recorded at scan rate of 10 mV/s using an HOPG electrode. Additional experimental details are provided in the Experimental procedures.

The pH dependence of the reduction potential of rcBphF was determined from pH 5 to 10 by diluting the protein in a mixture of Good buffers. Over this range, the reduction potential was essentially independent of the pH (−8.2 mV/pH, $R^2 = 0.9$; Figure 4a). Above pH 8.0, the intensity of the CV signal decreased and the peak separation increased. Above pH 10.0, the signal was too weak to interpret. The reduction potential of rcBphF was weakly dependent on ionic strength, decreasing slightly with increasing ionic strength (Figure 4b). In contrast, the reduction potential of BedB is independent of ionic strength (*18*). No CV signals were detected above an ionic strength of 0.5 M.

Thermodynamics of Electron Transfer. For nonisothermal systems, the temperature coefficient, $dE°/dT$, is directly related to the reaction entropy, $\Delta S°_{rc}$, where n is the number of electrons involved in the reaction and F is the Faraday constant (96485 J V^{-1} mol^{-1}) (*42*).

$$\Delta S°_{rc} = S°_{red} - S°_{ox} = nF(dE°/dT)$$

The change of entropy for the complete cell reaction adjusted to the SHE scale, $\Delta S°$, can be calculated from the following relation (*42*),

$$\Delta S° = \Delta S°_{rc} - \Delta S°\,(H_2) = \Delta S°_{rc} - 65\ J\ K^{-1}\ mol^{-1}$$

The slope of a linear least-squares fit to the data, $dE°/dT$, was −0.22 mV K^{-1}, which corresponds to a $\Delta S°_{rc}$ of −21.2 J K^{-1} mol^{-1} and a $\Delta S°$ of −86.2 J K^{-1} mol^{-1}.

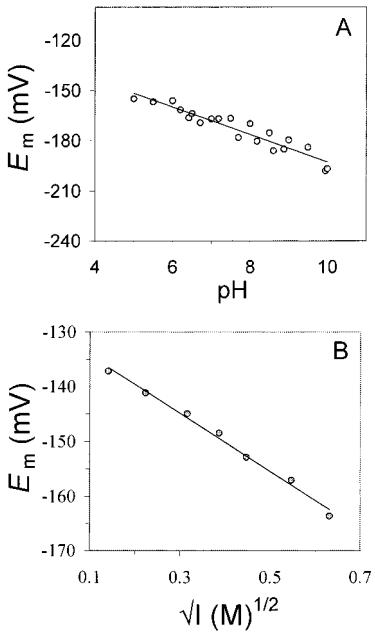

FIGURE 4: pH and ionic strength dependence of the reduction potential of rcBphF. (A) Cyclic voltammograms were recorded using a scan rate of 5 mV/s and a solution of Good's buffers (ionic strength of 0.1 M) at 23 °C. (B) Cyclic voltammograms were recorded using a scan rate of 10 mV/s and a solution of 20 mM MOPS, pH 7.0, containing different concentrations of KCl at 23 °C. Linear least squares best fits to the data are indicated.

The standard free energy change, $\Delta G° = 14.9$ kJ mol^{-1}, was calculated from $E°$ at 25.0 °C using the equation

$$\Delta G° = - nFE°$$

and the standard enthalpy change, $\Delta H° = -10.8$ kJ mol^{-1}, was calculated from the corresponding $\Delta G°$ and $\Delta S°$ via

$$\Delta H° = \Delta G° + T\Delta S°$$

EPR Spectroscopy. Reduced rcBphF exhibited a rhombic EPR spectrum with $g_x = 1.82$, $g_y = 1.91$, and $g_z = 2.04$ at 4 K (results not shown). These g values are very similar to those reported for other Rieske-type proteins (*3*, *18*).

Aggregation State of rcBphF in Solution. In the presence of 1 mM DTT, rcBphF eluted from a gel filtration column as a single Gaussian-shaped peak with an apparent molecular mass of 10.3 kDa (Figure 5). It was thus concluded that the protein is monomeric under these solution conditions. In contrast, after incubation of a 36 mg/mL solution of rcBphF for 4 h in the same buffer containing no DTT, a mixture of multimeric forms of the protein was detected by gel filtration, and less than 10% of rcBphF remained in the monomeric form (Figure 5). The two predominant forms of rcBphF had apparent molecular masses of 22.1 and 34.8 kDa, corresponding to dimers and trimers, respectively. Multimeric forms of rcBphF in these samples were also observed by electrospray ionization mass spectrometry analysis (results not shown), confirming the covalent nature of the protein−protein interactions. The addition of 5 mM DTT to a preparation of multimeric rcBphF resulted in the conversion of the protein to the monomeric form (96%) within 1 h (results not shown). Aggregation did not detectably affect the absorption spectra or reduction potential of rcBphF. Specifically, the midpoint reduction potential of a preparation

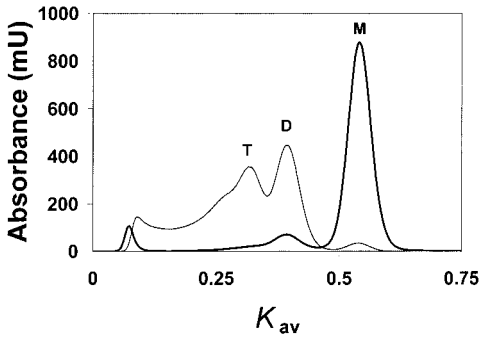

FIGURE 5: Dependence of elution profile of rcBphF from a gel filtration column on the presence of DTT. Chromatography was performed using a calibrated column as described in the Experimental Procedures in the presence (thick trace) and absence (thin trace) of 1 mM DTT (20 mM MOPS, pH 7.0, 0.15 M NaCl). Traces were recorded at 326 nm. Monomeric (M), dimeric (D), and trimeric (T) forms of rcBphF are identified.

of multimeric rcBphF was −154.5 mV vs SHE (20 mM MOPS and 80 mM KCl, pH 7.0, 22 °C), which is within 3 mV of that of a preparation of monomeric rcBphF. Moreover, the *R*-factor of the monomeric and multimeric forms were within 5% of each other, indicating that the fractions contained similar proportions of polypeptide and [Fe_2S_2] cluster.

Crystallographic Results. Diffraction patterns from several crystals were evaluated. 1.9 Å was the maximum resolution observed by the use of a rotating-anode X-ray source. The diffraction patterns were consistent with a primitive orthorhombic cell with parameters $a = 76.3$ Å, $b = 52.6$ Å, $c = 65$ Å. Analysis of systematic absences suggested the space group was either $P2_12_12$ or $P22_12$; subsequent experiments with synchrotron radiation (*20*) established that it was $P2_12_12$. On the basis of the mass-to-volume ratio (Matthews coefficient, *44*), it was determined that the asymmetric unit should contain two ($V_M = 2.7$ Å^3/Da) or possibly three ($V_M = 1.81$ Å^3/Da) monomers. Because of the possible space groups and the packing density, the presence of a 2-fold symmetric crystallographic or noncrystallographic dimer could not be excluded by the preliminary diffraction data. This is a signficant issue because the formation of a solution-phase dimer might bury the cluster.

Subsequent analysis of the crystal structure (*20*) established the asymmetric unit of the crystal includes two BphF molecules, A and B, related by noncrystallographic 2-fold symmetry. However, only 285 Å^2 is buried by this contact, which makes it very unlikely that the dimer would persist in solution. Moreover, if it were to persist, it would not affect the exposure of either cluster. The interactions established about crystallographic 2-folds are even less extensive and also do not affect cluster exposure.

Nevertheless, the clusters of molecules A and B are occluded by essentially identical crystal packing contacts, A with A′ and B with B′, generated by screw-axial symmetry as illustrated in Figure 6. The A−A′ contact buries 790 Å^2 of accessible surface area, whereas the B−B′ contact buries 870 Å^2. The possible relevance of these contacts to a solution-phase dimer is discussed below.

DISCUSSION

We established an efficient expression system for rcBphF, a recombinant Rieske-type ferredoxin involved in the microbial catabolism of biphenyl. Rapid purification under

FIGURE 6: Three molecules of rcBphF interacting in the head-to-tail fashion observed in the crystallographic fiber. The solid line represents the 2_1 screw axis along which the crystallographic fiber is propagated.

anaerobic conditions yielded 15 mg of a highly homogeneous preparation of the protein from 1 L of cell culture. This preparation yielded crystals of rcBphF for high-resolution crystallographic studies. The rhombic EPR spectrum of reduced rcBphF is highly characteristic of the EPR spectra of Rieske-type iron sulfur centers (*3*). Furthermore, the midpoint reduction potential of the rcBphF is typical of those of other small, soluble Rieske-type ferredoxin components of aromatic-ring dihydroxylating dioxygenases (*18*). The *R*-value of this preparation of rcBphF indicates that it has a slightly higher cluster content than BphF purified aerobically from *Burkholderia* sp. strain LB400 (*44*). Purified rcBphF transfers electrons efficiently from the reductase to the terminal oxygenase of biphenyl dioxygenase in vitro (*45*).

The spectroscopic and electrochemical properties of rcBphF are especially similar to those of BedB. The results from CD experiments are noteworthy because CD spectroscopy is a sensitive probe of cluster environment in iron sulfur proteins. For example, the CD spectra of oxidized HiPIPs I and II of *Ectothiorhodospira vacuolata*, each of which contains an $[Fe_4S_4]$ cluster, differ in the visible region notwithstanding their 65% sequence identity (*46*). Moreover, the substitution of a single aromatic residue within 5 Å of the cluster perturbs the spectra of reduced *E. halophila* HiPIP I (*47*). By analogy to what is observed in hemeproteins, $\pi \rightarrow \pi^*$ transitions of aromatic residues up to 15 Å from the cluster can be expected to influence electronic transitions of the latter through a coupled oscillator mechanism (*48*). Consistent with the very similar CD spectra of rcBphF and BedB (*18*), sequence alignments (not shown) and the structure of rcBphF (*20*) indicate that aromatic residues within 10 Å of the cluster in rcBphF are conserved in BedB. A notable exception is Met 67, which is immediately adjacent to the cluster ligand His 66 and whose β-carbon is 6.2 Å from a bridging sulfide of the cluster. It is possible that this residue, which is phenylalanine in BedB, is oriented such that it does not influence the electronic transitions of the cluster.

The multimerization of rcBphF observed in the absence of DTT is presumably due to the formation of intermolecular disulfide bonds. In particular, the similar *R*-factors of monomeric and multimeric rcBphF indicate that multimerization is not caused by a small fraction of the purified preparation that has lost its cluster. The observation of oligomeric states higher than the dimer suggests that more than one cysteine residue is involved in this multimerization. Other than the two cysteinyl cluster ligands, rcBphF contains cysteines at positions 7, 71, and 83 that could participate in intermolecular disulfides. BedB contains cysteines at positions that correspond to 30, 71, and 83. Multimerization has not been reported in BedB, presumably because this protein was purified in the presence of DTT (*49*). However, due to the propensity of rcBphF to form multimers, precautions were taken so that the reported biophysical properties of the protein reflect those of the monomer. Interestingly, variants of rcBphF in which any one of these residues was replaced by serine were not detectably expressed in *E. coli* (results not shown).

The electrochemical properties of the Rieske-type ferredoxins, as exemplified by BedB and BphF, differ from those of the Rieske proteins from the bc_1 and b_6f complexes in at least two important aspects. First, the reduction potentials of the former are about 450 mV lower than those of the latter. Second, the reduction potential and spectral characteristics of BedB and rcBphF are relatively independent of pH. This contrasts to the strong pH dependence of the reduction potential and CD spectra of the soluble fragment of the bc_1 Rieske protein (*21*, *50*). It has been proposed that these variations arise from differential exposure of the clusters to solvent in the two classes of proteins. For example, the pH-dependent behavior of the bc_1 fragment has been attributed to changes in the protonation of the cluster's histidinyl ligands, which are exposed to the solvent in the crystal structure (*12*). The contrasting, pH-independent behavior of BedB has been interpreted as an indication that its histidinyl ligands are buried from the solvent (*18*).

The crystal structure of rcBphF reveals that the exposure of the cluster's histidinyl ligands of any monomer is very similar to that in the soluble fragment of the bc_1 Rieske protein (*20*). However, in crystals of rcBphF, these ligands are involved in a protein−protein interaction that would reduce solvent exposure were it to occur in solution. As has been noted, the asymmetric unit contains two BphF molecules, one of type A and one of type B. The crystal consists of alternating layers of A-type and B-type molecules. Each layer is built of fibers of strongly interacting molecules propagated by a 2_1 screw axes parallel to the crystallograhic *b* axis (Figure 6). Within the fibers of either A or B

molecules, the cluster end of molecule *i* tucks into the side of molecule $i + 1$. This "head-to-tail" interaction is extremely similar in the A- and B-type fibers, although similarity is not required by crystallographic symmetry. The highly hydrated protein−protein interface is stabilized by two direct hydrogen bonds: one between Nϵ2 of His66 (i) and the backbone carbonyl of Arg73 ($i + 1$); and another between the backbone carbonyl of Leu65 (*i*) and Oη of Tyr106 ($i + 1$) (*20*). Free cysteine residues of the two monomers are not juxtaposed by this interaction: the closest approach between two Sγ atoms is 17.6 Å.

In light of the "head-to-tail" interaction between BphF molecules in the crystal, one might argue that the ferredoxin exists as a dimer in solution and that the histidinyl ligands are partially sequestered from the solvent. However, several lines of evidence indicate that the crystallographic interactions do not represent BphF's behavior in solution. First, the area of interaction is sparse and the interface is highly hydrated, which are characteristics of crystal contacts unlikely to persist in solution (*51*). Second, the interacting BphF molecules do not constitute a point-group-symmetric dimer or any other closed structure that would be compatible with a solution-phase oligomer. Instead, they form a fiber that extends throughout the crystal; within any given dimeric unit of this fiber, there is a free head on one monomer and a free tail on the other, giving rise to two different cluster environments. More importantly, the covalent oligomerization of rcBphF that occurs under certain solution conditions, is reversed by the addition of DTT and is thus unrelated to the noncovalent crystallographic interactions. Finally, the oligomerization state of rcBphF did not significantly influence the latter's reduction potential.

The relatively low, pH-independent reduction potentials of dioxygenase-associated ferredoxins has been attributed to the shielding of the FeS cluster and its ligands from the solvent (*18*). More recently, it has been suggested that this shielding might be achieved by dimerization of the ferredoxin in solution (*19*). The current results indicate that the reported biophysical properties of dioxygenase-associated ferredoxins reflect those of the monomeric form. Taken together with the crystallographic structure of rcBphF (*20*), we conclude that the strikingly different electrochemical properties of the Rieske clusters of dioxygenase-associated ferredoxins and mitochondrial bc_1 complexes are not due to differences in the solvent exposure of the clusters. Indeed, comparison of the structures of the cluster binding domains of these proteins suggests that the electrochemical differences are determined principally by the orientation and position of protein dipoles around the cluster.

ACKNOWLEDGMENT

Giuseppe Terracina is thanked for his contributions to crystallization and preliminary diffraction experiments.

REFERENCES

1. Beinert, H., Holm, R., and Münck, E. (1997) *Science 277*, 653−659.
2. Stephens, P. J., Jollie, D. R., and Warshel, A. (1996) *Chem. Rev. 96*, 2491−2513.
3. Rieske, J. S., Hansen, R. E., and Zaugg, W. S. (1964) *J. Biol. Chem. 239*, 3017−3021.
4. Bowyer, J. R., Dutton, P. L., Prince, R. C., and Crafts, A. R. (1980) *Biochim. Biophys. Acta 592*, 445−460.
5. Meinhardt, S. W., Yang, W. H., Trumpower, B. L., and Ohnishi, T. (1987) *J. Biol. Chem. 262*, 8702−8706.
6. Nelson, N., and Neuman, N. (1972) *J. Biol. Chem. 247*, 1817−1824.
7. Butler, C. S., and Mason, J. R. (1997) *Adv. Microbiol. Physiol. 38*, 47−84.
8. Gubriel, R. J., Batie, C. J., Sivaraja, M., True, A. E., Fee, J. A., Hoffman, B. M., and Ballou, D. P. (1989) *Biochemistry 28*, 4861−4871.
9. Gubriel, R. J., Ohnishi, T., Robertson, D. E., Daldal, F., and Hoffman, B. M. (1991) *Biochem. 30*, 11579−11584.
10. Gubriel, R. J., Doan, P. E., Gassner, G. T., Macke, T. J., Case, D. A., Ohnishi, T., Fee, J. A., Ballou, D. P., and Hoffman, B. M. (1996) *Biochemistry 35*, 7834−7845.
11. Britt, R. D., Sauer, K., Klein, M. P., Knaff, D. B., Kriauciunas, A., Yu, C.-A., Yu, L., and Malkin, R. (1991) *Biochemistry 30*, 1892−1901.
12. Iwata, S., Saynovits, M., Link, T. A., and Michel, H. (1996) *Structure 4*, 567−579.
13. Carrell, C. J., Zhang, H., Cramer, W. A., and Smith, J. L. (1997) *Structure 5*, 1613−1625.
14. Fee, J. A., Findling, K. L., Yoshida, T., Hille, R., Tarr, G. E., Hearshen, D. O., Dunham, W. R., Day, E. P., Kent, T. A., and Münck, E. (1984) *J. Biol. Chem. 259*, 124−133.
15. Gibson, J. F., Hall, D. O., Thornley, J. H. M., and Whatley, F. R. (1966) *Proc. Natl. Acad. Sci. U.S.A. 56*, 987−990.
16. Geary, P. J., Saboowalla, F., Patil, D., and Cammack, R. (1984) *Biochem. J. 217*, 667−673.
17. Kauppi, B., Lee, K., Carredano, E., Parales, R. E., Gibson, D. T., Eklund, H., and Ramaswamy, S. (1998) *Structure 6*, 571−586.
18. Link, T. A., Hatzfeld, O. M., Unalkat, P., Shergill, J. K., Cammack, R., and Mason, J. R. (1996) *Biochemistry 35*, 7546−7552.
19. Link, T. A. (1999) *Adv. Inorg. Chem. 47*, 83−157.
20. Colbert, C. L., Couture, M. M. J., Eltis, L. D., and Bolin, J. T. (2000) *Structure 8*, (in press).
21. Link, T. A., Hagen, W. A., Pierik, A. J., Assmann, C., and von Jagow, G. (1992) *Eur. J. Biochem. 208*, 685−691.
22. Zhang, H., Carrell, C. J., Huang, D., Sled, V., Ohnishi, T., Smith, J. L. and Cramer, W. A. (1996) *J. Biol. Chem. 271*, 31360−31366.
23. Erickson, B. D., and Mondello, F. J. (1992) *J. Bacteriol. 174*, 2903−2912.
24. Studier, F. W. and Moffatt, B. A. (1986) *J. Mol. Biol. 189*, 113−130.
25. Borck, K., Beggs, J. D., Brammar, W. J., Hopkins, A. S., and Murray, M. E. (1976) *Mol. Gen. Genet. 146*, 199−207.
26. Tabor, S., and Richardson, C. C. (1985) *Proc. Natl. Acad. Sci. U. S. A. 82*, 1074−1078.
27. Hofer, B., Eltis, L. D., Dowling, D. N., and Timmis, K. N. (1993) *Gene 130*, 47−55.
28. Eltis, L. D., Iwagami, S. G., and Smith, M. (1994) *Protein Eng. 7*, 1145−1150.
29. Bauchop, T., and Elsden, R. (1960) *J. Gen. Microbiol. 23*, 457−469.
30. Bertini, I., Couture, M. M.-J., Donaire, A., Eltis, L. D., Felli, I. C., and Luchinat, C. (1996) *Eur. J. Biochem. 241*, 440−452.
31. Ausubel, F. M., Brent, R., Kingston, R. E., Moore, D. D., Seidman, J. G., Smith, H. A., and Struhl, K. (1991) *Current protocols in molecular biology*, Greene Publishing Associates, New York.
32. Schäger, H., and von Jagow, G. (1987) *Anal. Biochem. 166*, 368−379.
33. Bradford, M. M. (1976) *Anal. Biochem. 72*, 248−254.
34. Haigler, B. E., and Gibson, D. T. (1990) *J. Bacteriol 172*, 457−464.
35. Chen, J.-S., and Morenson, L. E. (1997) *Anal. Biochem. 79*, 157−165.

36. Maurus, R., Overall, C. M., Bogumil, R., Luo, Y., Mauk, A. G., Smith, M., and Brayer, G. D. (1997) *Biochim. Biophys. Acta 1341*, 1−13.
37. Hagen, W. (1989) *Eur. J. Biochem. 182*, 523−530.
38. Otwinowski, Z., and Minor, W. (1997) *Methods Enzymol. 276*, 307−326.
39. CCP4 (1994) *Acta Crystallogr., Sect. D 50*, 760−763.
40. Nicholson, R. S. (1965) *Anal. Chem. 37*, 1351−1355.
41. Reid, L. S., Taniguchi, V. T., Gray, H. B., and Mauk A. G. (1982) *J. Am. Chem. Soc. 104*, 7516−7519.
42. Taniguchi, V. T., Sailasuta-Scott, N., Anson, F. C., and Gray, H. B. (1980) *Pure Appl. Chem. 52*, 2275−2281.
43. Matthews, B. W. (1977) in *The Proteins*, 3rd ed., Vol. III, pp 403−590, H. Neurath and R. L Hill, Eds., Academic Press, New York.
44. Haddock, J. D., Pelletier, D. A., and Gibson, D. T. (1997) *J. Indust. Microbiol. Biotech. 19*, 355−359.
45. Imbeault, N. Y. R., Powlowski, J. B., Colbert, C. L., Bolin, J. T., and Eltis, L. D. (2000) *J. Biol. Chem. 275*, 12430−12437.
46. Przysiecki, C. T., Meyer, T. E., and Cusanovich, M. A. (1985) *Biochemistry 24*, 2542−2549.
47. Iwagami, S. G., Creagh, A. L., Haynes, C. A., Borsari, M., Felli, I. C., Piccioli, M., and Eltis, L. D. (1995) *Protein Sci. 4*, 2562−2572.
48. Hsu, M. C., and Woody, R. W. (1971) *J. Am. Chem. Soc. 93*, 3515−3525.
49. Crutcher, S. E., and Geary, P. J. (1979) *Biochem. J. 177*, 393−400.
50. Link, T. A. (1994) *Biochim. Biophys. Acta 1185*, 81−84.
51. Janin, J., and Rodier, F. (1995) *Proteins 23*, 580−587.

BI001780R